Environmental Science and Pollution Research (2023) 30:89479–89494
https://doi.org/10.1007/s11356-023-28747-8

RESEARCH ARTICLE

The protective effects of chrysin on cadmium-induced pulmonary toxicity; a multi-biomarker approach

Nurhan Akaras[1] · Mustafa Ileriturk[2] · Cihan Gur[3] · Sefa Kucukler[3] · Mehmet Oz[4] · Fatih Mehmet Kandemir[5]

Received: 18 April 2023 / Accepted: 7 July 2023 / Published online: 15 July 2023

Abstract

This study aimed to determine the potential protective effects of chrysin (CHR) on experimental cadmium (Cd)-induced lung toxicity in rats. To this end, rats were divided into five groups; Control, CHR, Cd, Cd + CHR25, Cd + CHR50. In the study, rats were treated with CHR (oral gavage, 25 mg/kg and 50 mg/kg) 30 min after giving Cd (oral gavage, 25 mg/kg) for 7 consecutive days. The effects of Cd and CHR treatments on oxidative stress, inflammatory response, ER stress, apoptosis and tissue damage in rat lung tissues were determined by biochemical and histological methods. Our results revealed that CHR therapy for Cd-administered rats could significantly reduce MDA levels in lung tissue while significantly increasing the activity of antioxidant enzymes (SOD, CAT, GPx) and GSH levels. CHR agent exerted antiinflammatory effect by lowering elevated levels of NF-κB, IL-1β IL-6, TNF-α, RAGE and NRLP3 in Cd-induced lung tissue. Moreover CHR down-regulated Cd-induced ER stress markers (PERK, IRE1, ATF6, CHOP, and GRP78) and apoptosis markers (Caspase-3, Bax) lung tissue. CHR up-regulated the Bcl-2 gene, an anti-apoptotic marker. Besides, CHR attenuated the side effects caused by Cd by modulating histopathological changes such as hemorrhage, inflammatory cell infiltration, thickening of the alveolar wall and collagen increase. Immunohistochemically, NF-κB and Caspase-3 expressions were intense in the Cd group, while these expressions were decreased in the Cd + CHR groups. These results suggest that CHR exhibits protective effects against Cd-induced lung toxicity in rats by ameliorating oxidative stress, inflammation, apoptosis, endoplasmic reticulum stress and histological changes.

Keywords Apoptosis · Cadmium · Chrysin · Inflammation · Lung injury · Endoplasmic reticulum stress

Introduction

Heavy metals have emerged as a major global concern as a result of rapid industrialization and urbanization (Poli et al. 2022). Cadmium (Cd) is one of the most significant heavy metals that has the potential to be an environmental and occupational pollutant, posing a serious hazard to human health (Dashtbanei & Keshtmand 2022, El-Ebiary et al. 2016; Guo et al. 2022; Cao et al. 2022). Cd enters living organisms' bodies through food, water, occupational inhalation and skin (Zhu et al. 2019; Zhang et al. 2021). Even in trace amounts, Cd, which is not physiologically necessary in the human body, is extremely toxic to the body (Elkin et al. 2022; Yesildag et al. 2022). The body of a person weighing 70 kg is exposed to 25–60 µg of Cd through daily food intake and 0.1–0.2 µg of Cd through smoking. Hence, even non-smokers who are not occupationally exposed to Cd face unavoidable risk (Zhu et al. 2019). Also, in the general non-smoking population, less than 10% of total Cd exposure occurs through inhalation of ambient air and drinking water. Furthermore, this metal has a biological half-life of 10–30 years and its low excretion rate is a major reason for its potential risk (Kulas et al. 2021). Epidemiologic data show that exposure to Cd causes severe damage to many organs, including nephrotoxicity, hepatotoxicity

Responsible Editor: Mohamed M. Abdel-Daim

✉ Nurhan Akaras
nurakaras@hotmail.com

[1] Department of Histology and Embryology, Faculty of Medicine, Aksaray University, Aksaray, Turkey

[2] Department of Animal Science, Horasan Vocational College, Atatürk University, Erzurum, Turkey

[3] Department of Biochemistry, Faculty of Veterinary Medicine, Atatürk University, Erzurum, Turkey

[4] Department of Physiology, Faculty of Medicine, Aksaray University, Aksaray, Turkey

[5] Department of Medical Biochemistry, Faculty of Medicine, Aksaray University, Aksaray, Turkey

and pneumotoxicity (Gao et al. 2017; Kandemir et al. 2021). Exposure to low levels of Cd can cause damage to the skeletal system, hemopoietic system, and cardiovascular system, as well as impaired vision and hearing. Besides the strong teratogenic and mutagenic effects associated with cadmium, low doses exert adverse effects on both human male and female reproduction and affect pregnancy or its outcome (Genchi et al. 2020, Jarup et al. 2003). In addition, Cd and its compounds were classified as a type 1 carcinogen for humans by the International Agency for Research on Cancer in 1993 (Zhou et al. 2016). Specifically, inhalation and oral exposure to Cd leads to Cd accumulation in the lung, posing a risk to the lung. When lung tissue, which is highly susceptible to its external environment, is exposed to Cd for a long term, it causes respiratory diseases such as pneumonia, chronic obstructive pulmonary disease (COPD), chronic cough, bronchitis, asthma, lung cancer, tuberculosis, and pulmonary emphysema (Naidoo et al. 2019; Rafiei-Asl et al. 2021).

Cd exposure causes necroptosis, apoptosis, and autophagy damage through various mechanisms such as increased Reactive Oxygen Species (ROS) production and inhibition of antioxidant enzyme activity (Zhang et al. 2023). Although the precise mechanisms of the harmful effects of Cd toxicity on tissues are not yet fully understood, one of the most widely accepted mechanisms is the excessive triggering of free radical generation, leading to oxidative stress (Wang et al. 2019). The accumulation of ROS by Cd exposure triggers oxidative stress and leads to organ toxicity by damaging proteins, lipids and nucleic acids (Noor et al. 2022). There have also been studies showing that Cd causes defects in gene expression and this effect alters the expression of genes in the target organ of focus (Dashtbanei & Keshtmand 2022, Elkin et al. 2022; Pan et al. 2021). Besides, reports reveal that Cd has pro-inflammatory properties and damages vital organelles like endoplasmic reticulum and mitochondria, resulting in cell apoptosis (Dashtbanei & Keshtmand 2022, Rafiei-Asl et al. 2021; Wang et al. 2022). A therapeutic approach is therefore urgently needed to delay or halt the progression of all these harmful effects of exposure to Cd.

Chelation therapies have gained importance in patients with Cd exposure and in experimental studies in recent years (El-Ebiary et al. 2016). Chelation of redox-active metal ions, DNA repair, regulation of gene expression, free radical scavenging, anticancer and antiinflammatory effects of some medicinal plants and phytochemicals have been described, particularly in the twenty-first century (Gao et al. 2017; Seydi et al. 2019; Yesildag et al. 2022).

Chrysin (CHR, (5,7-dihydroxy-2-phenyl-4H-chromene-4-one or 5,7-dihydroxyflavone, Fig. 1), a natural flavonoid, is a phytochemical with 5,7-dihydroxyl structure. It is abundant in nature, especially in honey, propolis, some flowers (*Passiflora caerulea, Passiflora incarnata*) and mushrooms (Kandemir et al. 2017; Kucukler et al. 2021; Varışlı et al. 2023). CHR, which has no adverse effects, possesses various pharmacological effects that are beneficial to health including antioxidant, antiinflammation, anticancer, antiallergic, antiaging, antidiabetic and antiapoptotic (Aksu et al. 2018; Ileriturk et al. 2021). Structurally, CHR has two benzene rings (A & B) and an oxygen-containing heterocyclic ring. It has 2–3 double bonded carbons with a carbonyl group attached to the 4th carbon, while the 3-carbon hydroxyl group is absent. Also, the 5th and 7th carbon atoms contain -OH groups. Unlike various flavonoids, chrysin does not share any oxygenation in Ring-B. Mainly, the variation in A-ring oxygenation is responsible for various crisscross derivatives such as wogonin, baicalein, and oroxylin A. The biological activities of chrysin are associated with the absence of oxygenation in the B and C rings, accompanied by antiinflammatory and antitoxic effects. The antioxidant activity of different flavones is also predicted to depend on the structural diversity of these chemical entities. The presence of the carbonyl group on C-4 and a double bond (30,40 hydroxylation) between C-2 and C3 is mainly associated with the antioxidant activity of chrysin (Talebi et al. 2021; Naz et al. 2019). To the best of our knowledge, however, the role of CHR in pulmonary toxicity after Cd exposure has not been investigated in the literature. The aim of this study was to investigate the antioxidant, antiapoptotic, and antiinflammatory effects of CHR against Cd-induced lung toxicity in rats by molecular, biochemical, and histological methods.

Material and method

Drugs and chemicals

Cd (CAS No. 7440–43-9, 99.99% purity), CHR (cas no: 480–40-0,97% purity) and all other chemicals were of analytical purity and were obtained from Sigma-Aldrich and Merck (St. Louis, MO, US).

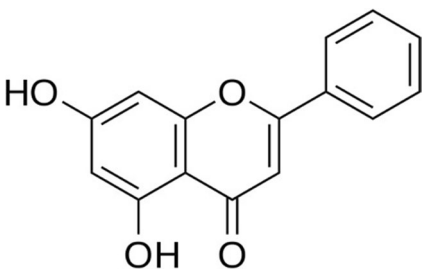

Fig. 1 Chemical structure of chrysin

Experimental design

In this study, 35 male *Wistar albino* rats weighing 220–250 g purchased from Necmettin Erbakan University KONÜDAM Experimental Medicine Application and Research Center were employed. All animals were kept under appropriate laboratory conditions (25 ± 1 °C, 50 ± 5% humidity and 12:12 h light/dark cycle) until the last day of the experiment. Animals were fed ad libitum with water and a standard laboratory chow throughout the study. The study was approved by Necmettin Erbakan University Animal Experiments Local Ethics Committee (no.2022–55). Before the experiment began, all animals were randomly divided into five groups of 7 rats in each. The number of animals in the groups was determined according to the previous study (Yesildag et al. 2022). The dose of Cd and CHR used in the experiment were administered based on the previous studies (Hanedan et al. 2018; Kandemir et al. 2021; Temel et al. 2021). Groups;

1. Control Group: Saline was given by gastric gavage for 7 days.
2. Chrysin (CHR) Group: CHR was given by gastric gavage at a dose of 50 mg/kg for 7 days.
3. Cadmium (Cd) Group: Cd was given by gastric gavage at a dose of 25 mg/kg for 7 days.
4. Cadmium + Chrysin 25 (Cd + CHR25) Group: Cd was given by gastric gavage at a dose of 25 mg/kg (1 time/day for 7 days). Half an hour after Cd administration, CHR was given by gastric gavage at a dose of 25 mg/kg (1 time/day for 7 days).
5. Cadmium + Chrysin 50 (Cd + CHR50) Group: Cd was given by gastric gavage at a dose of 25 mg/kg (1 time/day for 7 days). Half an hour after Cd administration, CHR was given by gastric gavage at a dose of 50 mg/kg (1 time/day for 7 days).

The rats were sacrificed under mild sevoflurane anesthesia 24 h after the last drug administration (8^{th} day of the experiment) and their lungs were removed at the end of the experiment. Part of the tissues were stored at -20 °C for biochemical analyses and the other part was stored in 10% formalin solution for immunohistochemical and histopathological evaluations.

The analysis of oxidative stress markers

A homogenizer (Tissue Lyser II) and 1.15% potassium chloride (KCl) buffer were utilized to homogenize the lung tissues. To obtain the supernatant, homogenates were centrifuged for SOD, CAT and MDA assays at 3.500 rpm at 4 °C for 15 min and other homogenates at 10.000 rpm at 4 °C for 20 min. MDA levels were measured in nmol/g tissue using the method of Placer et al (1966). This method is based on measuring the color formed as a result of the reaction of MDA with TBA at a wavelength of 532 nm. Superoxide dismutase (SOD) activity was measured by the method of Sun et al. (1988) and presented as U/g protein. This method is based on the nitroblue tetrazolium (NBT) degradation of the superoxide radical produced by the xanthinoxanthine oxidase system and formazan. SOD activity was measured as the level of inhibition of absorbance at 560 nm. CAT activity was measured using the Aebi (Aebi 1984) protocol and expressed as Catal/g protein. In this method, catalase activity was determined by spectrophotometric measurement of the amount of hydrogen peroxide consumed per unit time. GSH and GPx were measured by the method used by Sedlak and Lindsay (1968), Lawrence and Burk (1976), respectively. GSH was expressed as nmol/g tissue and GPx as U/g protein. GSH content of the lungs was measured at 412 nm. Total protein content of lung tissue homogenates was measured by the method of Lowry et al (1951).

The analysis of real-time polymerase chain reaction (RT-PCR)

Rat lung tissues were treated with QIAzol Lysis Reagent (79,306; Qiagen) and total RNA was isolated from tissues. The total RNA contents of all groups were equalized after measuring total RNA concentrations with NanoDrop (BioTek Epoch). These were then converted into double-stranded structures (cDNA) via the iScript cDNA Synthesis Kit (Bio-Rad) according to the temperatures and time periods given by manufacturer. The cDNAs obtained were used to analyze the relative mRNA transcript levels of Nuclear Factor kappa B (NF-κB), Interleukin-1 beta (IL-1β), Interleukin-6 (IL-6), Tumor necrosis factor-alpha (TNF-α), NLR Family Pyrin Domain Containing 3 (NLRP3), Receptor for Advanced Glycation Endproducts (RAGE) for inflammation damage level analysis; Protein Kinase RNA-Like ER Kinase (PERK), Activating transcription factor 6 (ATF-6), Inositol-requiring enzyme 1 (IRE1), CCAAT-enhancer-binding protein homologous protein (CHOP) and Glucose-regulated protein 78 (GRP-78) for endoplasmic reticulum stress damage analysis; cysteine-aspartic acid protease (Caspase-3), Bax, B-cell lymphoma 2 (Bcl-2) for apoptosis damage level (sequences presented in Table 1). To this end, a mixture of primers of the genes (including β-Actin), iTaq Universal SYBR Green Supermix (BIORAD) and cDNAs was prepared in the ratios specified by the manufacturer, and then the reaction was performed in Rotor-Gene Q (Qiagen) at the set time and temperature cycles according to the procedure provided by the manufacturer. After the cycles were completed, CT values were normalized to β-Actin by the $2^{-\Delta\Delta CT}$ method (Livak & Schmittgen 2001). The reason for using β-Actin is that its stability in lung tissue has been demonstrated in previous studies (Sharaf El-Din and Abd Allah 2016, Liu et al. 2017, Arafa et al. 2015).

Table 1 Primer sequences

Gene	Sequences (5'-3')	Length (bp)	Accession No
NF-κB	F: AGTCCCGCCCCTTCTAAAAC R: CAATGGCCTCTGTGTAGCCC	106	NM_001276711.1
IL-6	F: AGCGATGATGCACTGTCAGA R: GGAACTCCAGAAGACCAGAGC	127	NM_012589.2
IL-1β	F: ATGGCAACTGTCCCTGAACT R: AGTGACACTGCCTTCCTGAA	197	NM_031512.2
TNF-α	F: CTCGAGTGACAAGCCCGTAG R: ATCTGCTGGTACCACCAGTT	139	NM_012675.3
NLRP3	F: TCCTGCAGAGCCTACAGTTG R: GGCTTGCAGCACTGAAGAAC	185	NM_001191642.1
RAGE	F: CTGAGGTAGGGCATGAGGATG R: TTCATCACCGGTTTCTGTGACC	113	NM_053336.2
Caspase-3	F: ACTGGAATGTCAGCTCGCAA R: GCAGTAGTCGCCTCTGAAGA	270	NM_012922.2
Bcl-2	F: GACTTTGCAGAGATGTCCAG R: TCAGGTACTCAGTCATCCAC	214	NM_016993.2
Bax	F: TTTCATCCAGGATCGAGCAG R: AATCATCCTCTGCAGCTCCA	154	NM_017059.2
PERK	F: GATGCCGAGAATCATGGGAA R: AGATTCGAGAAGGGACTCCA	198	NM_031599.2
ATF-6	F: TCAACTCAGCACGTTCCTGA R: GACCAGTGACAGGCTTCTCT	130	NM_001107196.1
IRE1	F: GCAGTTCCAGTACATTGCCATTG R: CAGGTCTCTGTGAACAATGTTGA	163	NM_001191926.1
CHOP	F: GAAGCCTGGTATGAGGATCT R: GAACTCTGACTGGAATCTGG	209	NM_001109986.1
GRP78	F: CATGCAGTTGTGACTGTACCAG R: CTCTTATCCAGGCCATATGCAA	143	NM_013083.2
β-Actin	F: CAGCCTTCCTTCTTGGGTATG R: AGCTCAGTAACAGTCCGCCT	360	NM_031144.3

Hematoxylin&Eosin (H&E) staining

Lung tissues taken for histopathological analysis were kept in formalin for 48 h for fixative purposes. In accordance with the tissue follow-up procedure, the lung tissue was dehydrated by passing through increasing degrees of alcohols, dehydration and transparency by being kept in xylol three times. After paraffin infiltration, the transparentized tissues were transformed into blocks. Five μm thick sections were taken from the paraffin blocks using a microtome. The sections were then stained with conventional Hematoxylin–Eosin (H&E). The stained lung tissues were examined using a binocular Olympus Cx43 light microscope (Olympus Inc., Tokyo, Japan) and photographed with an EP50 camera (Olympus Inc., Tokyo, Japan).

Masson's Trichrome staining

Five μm thick sections were taken from the paraffin blocks by routine tissue follow-up to the formalin-fixed lung tissues. The sections were stained with Masson's Trichrome to visualize collagen deposition (by passing through Weigert iron hematoxylin, picric acid alcoholic solution, poppy red fuchsin solution, phosphomolybdic acid solution, masson aniline blue solution, respectively). The stained lung tissues were examined using a binocular Olympus Cx43 light microscope (Olympus Inc., Tokyo, Japan) and photographed with an EP50 camera (Olympus Inc., Tokyo, Japan).

Immunohistochemical analysis

Tissue preparations prepared from approximately 3-μm-thick sections of lung tissue were deparaffinized by soaking in xylol and passed through a graded alcohol series. The preparations were then heat treated in ethylenediaminetetraacetic acid (EDTA) buffer (pH:8.0) for antigen retrieval. The preparations were then placed in 3% hydrogen peroxide solution to prevent the formation of endogenous peroxidase activity. After this, normal bovine serum was used to avoid nonspecific staining. The primary antibodies NF-kB (Santa Cruz Biotechnology, sc-8414) and Caspase-3 (Santa Cruz Biotechnology, sc-56053) were then applied to the preparations for one

hour and the preparations were then exposed to biotinylated secondary antibody and streptavidin horseradish peroxidase (Dako, Universal LSAB Kit, K0690) for 30 min. After this treatment, 3,3'-diaminobenzidine tetrahydrochloride (DAB, Thermo) solution was applied to the tissue preparations to visualize the reactions. Harris's haematoxylin stain was applied to stain the nuclei of the cells and the preparations were passed through graded ethanol series and xylol and covered with Entellan (Merck, German). Finally, they were randomly blinded by the investigators to assess the binding levels of antibodies. For immunohistochemical analysis of the results, the free ImageJ 1.51v 9 and Color Deconvolution plugin downloaded from the NIH website (//rsb.info.nih.gov/ij) were used. In terms of tissue immunoreactivity, at least 3 non-overlapping areas were evaluated in microphotographs taken from an average of three randomly selected non-consecutive histological sections per subject from each group.

The following formula was used to calculate the percentage of the density of positive cells (Kassab et al. 2020).

$$\text{Percentage of positive cells} = \text{Number of positive cells/Total counted cells} \times 100\ \left[400\ \text{magnification on DAB} - \text{stained slides}\right]$$

Statistical analysis

IBM SPSS was used to perform statistical evaluation of the findings obtained from testicular tissue analysis (version 20.0; IBM Co, North Castle, NY). To determine whether there were statistical differences between the experimental groups, one-way ANOVA and Tukey's post hoc tests were used. Each sample was run in triplicate in RT-PCR analyses, and the results are presented as mean SD. The values of $p<0.05$, $p<0.01$ and $p<0.001$ were considered statistically significant.

Results

Effects of Cd and CHR administrations on oxidative stress markers in lung tissue

The levels of oxidative stress markers analyzed in lung tissues of rats treated with Cd and CHR are given in Fig. 2. According to the data obtained, MDA levels increased 2.09-fold compared to the control group due to lipid peroxidation in the lung tissues of rats after Cd administration ($p<0.001$). On the other hand, it was determined that MDA levels decreased in a dose-dependent manner (low dose; 1.19-fold, high dose; 1.24-fold) with CHR treatment. Exposure to Cd significantly inhibited the activities of antioxidant enzymes SOD, CAT, and GPx, as well as reduced glutathione levels in rat lung tissue compared to the control group (SOD; 2.10-fold, CAT; 2,18-fold, GPx; 2.24-fold, GSH; 2.15-fold) ($p<0.001$). CHR administration, on the other hand, was ascertained to bring Cd-induced suppressed SOD (low dose; 1.35-fold, high dose; 1.57-fold), CAT (low dose; 1.30-fold, high dose; 1.60-fold), GPx (low dose; 1.19-fold, high dose; 1.48-fold) activities, and GSH levels (low dose; 1.53-fold, high dose; 1.89-fold) close to control values. CHR 50 mg dose was found to be more effective on Cd-induced oxidative stress damage.

Effects of Cd and CHR administrations on inflammation markers in lung tissue

The effects of Cd and CHR on mRNA transcript levels of inflammatory markers NF-κB, IL-1β, IL-6, TNF- α in rat lung tissues are shown in Fig. 3. Findings showed that Cd administration increased the expression of NF-κB, IL-1 β, IL-6, and TNF-α and caused inflammation ($p<0.001$). (According to the control group: NF-κB; 2.11-fold, IL-1β; 2.11-fold, TNF-α; 2.31-fold, IL-6; 1.72-fold). However, CHR administration exerted an anti-inflammatory effect by suppressing the expressions of NF-κB (low dose; 1.23-fold, high dose; 1.51-fold), IL-1β (low dose; 1.09-fold, high dose; 1.35-fold), IL-6 (low dose; 1.11-fold, high dose; 1.23-fold), and TNF-α (low dose; 1.13-fold, high dose; 1.44-fold). The 50 mg/kg CHR dose, on the other hand, was more effective on inflammation than the 25 mg/kg CHR dose.

Effects of Cd and CHR administrations on RAGE and NLRP3 gene expression levels in lung tissue

The effects of Cd and CHR on mRNA transcript levels of RAGE and NLRP3 in rat lung tissues are shown in Fig. 4. It was observed that Cd administration up-regulated RAGE and NLRP3 expressions in lung tissues) (According to the control group: RAGE; 1.74-fold, NLRP3; 1.63-fold) ($p<0.001$). On the other hand, RAGE and NLRP3 gene expression levels were lower in the Cd + CHR 25 (RAGE; 1.11-fold, NLRP3; 1.32-fold) and Cd + CHR 50 (RAGE; 1.22-fold, NLRP3; 1.48-fold) groups compared to the Cd group.

Effects of Cd and CHR administrations on ER-stress markers in lung tissue

The relative mRNA transcript levels of ER stress markers are presented in Fig. 5. According to the data, it appears that Cd causes ER stress in lung tissues and up-regulates ATF-6, PERK, IRE1, CHOP and GRP-78 genes (According to the control group: ATF-6; 1.77-fold, PERK; 1.69-fold, IRE1;

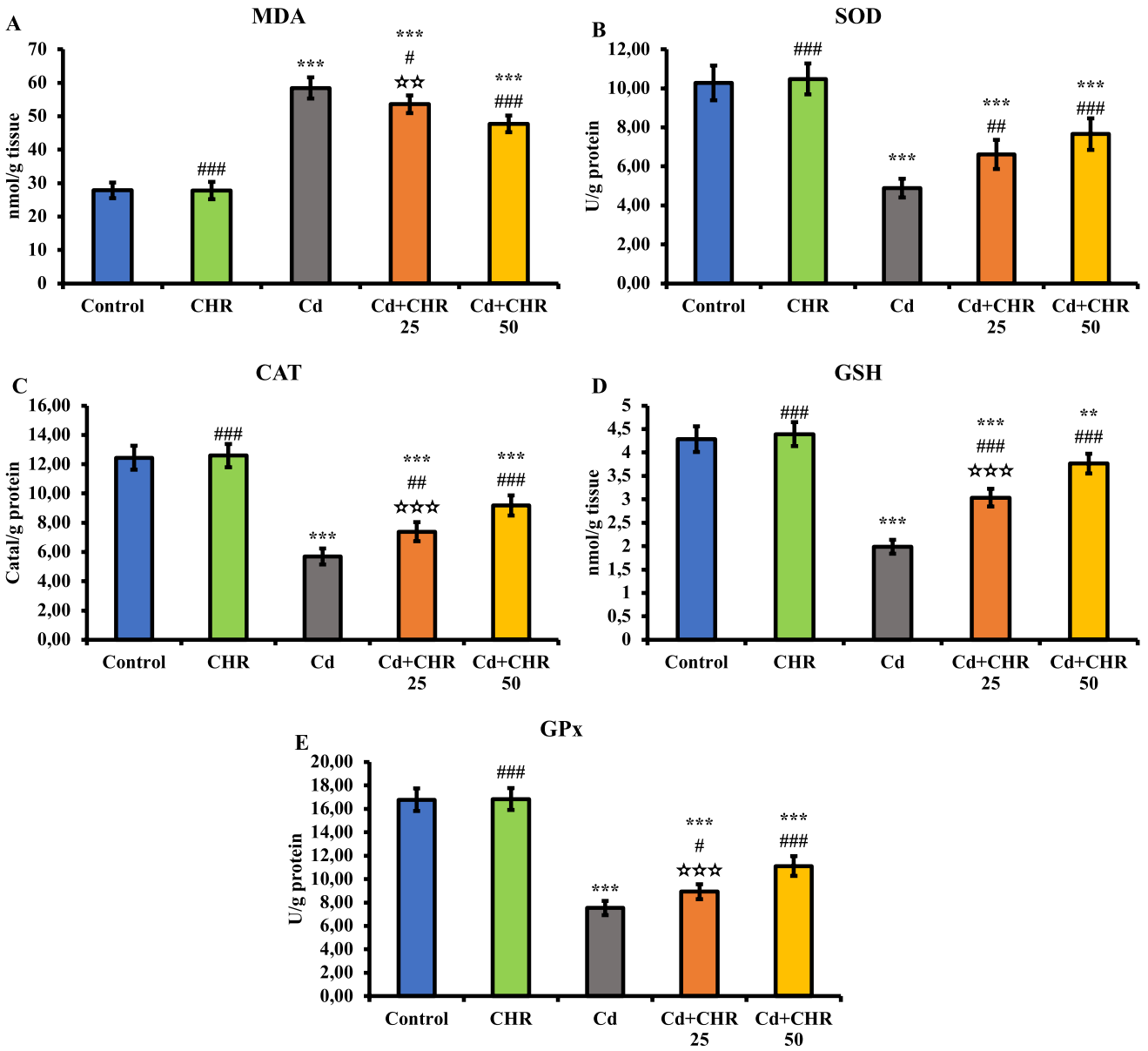

Fig. 2 Effects of Cd and CHR administration on oxidative stress markers in rat lung tissues. (MDA (Malondialdehyde), SOD (Superoxide dismutase), CAT (Catalase), GSH (Glutathione), GPx (Glutathione peroxidase)) Statistical significance (Control vs others: * $P < 0.05$, ** $p < 0.01$, *** $p < 0.001$, Cd vs others: $^{\#}$ $P < 0.05$, $^{\#\#}$ $p < 0.01$, $^{\#\#\#}$ $p < 0.001$, Cd + CHR 25 vs Cd + CHR 50: $^{\star}P < 0.05$, ** $p < 0.01$, *** $p < 0.001$) was analyzed using One Way ANOVA

1.64-fold, CHOP; 1.72-fold, GRP-78; 1.69-fold) ($p < 0.001$). The data also revealed that Cd administration in combination with CHR ameliorated ER stress by down-regulating PERK (low dose; 1.37-fold, high dose; 1.52-fold), IRE1 (low dose; 1.16-fold, high dose; 1.38-fold), ATF-6 (low dose; 1.25-fold, high dose; 1.41-fold), CHOP (low dose; 1.17-fold, high dose; 1.25-fold) and GRP-78 (low dose; 1.14-fold, high dose; 1.27-fold) gene expression levels.

Effects of Cd and CHR administrations on apoptosis markers in lung tissue

A summary of mRNA transcript levels of apoptotic markers is given in Fig. 6. It was found that Cd administration caused apoptosis by decreasing Bcl-2 expression (1.84-fold) and increasing Caspase-3 (2.35-fold) and Bax (1.85-fold) expression in lung tissue ($p < 0.001$). In addition,

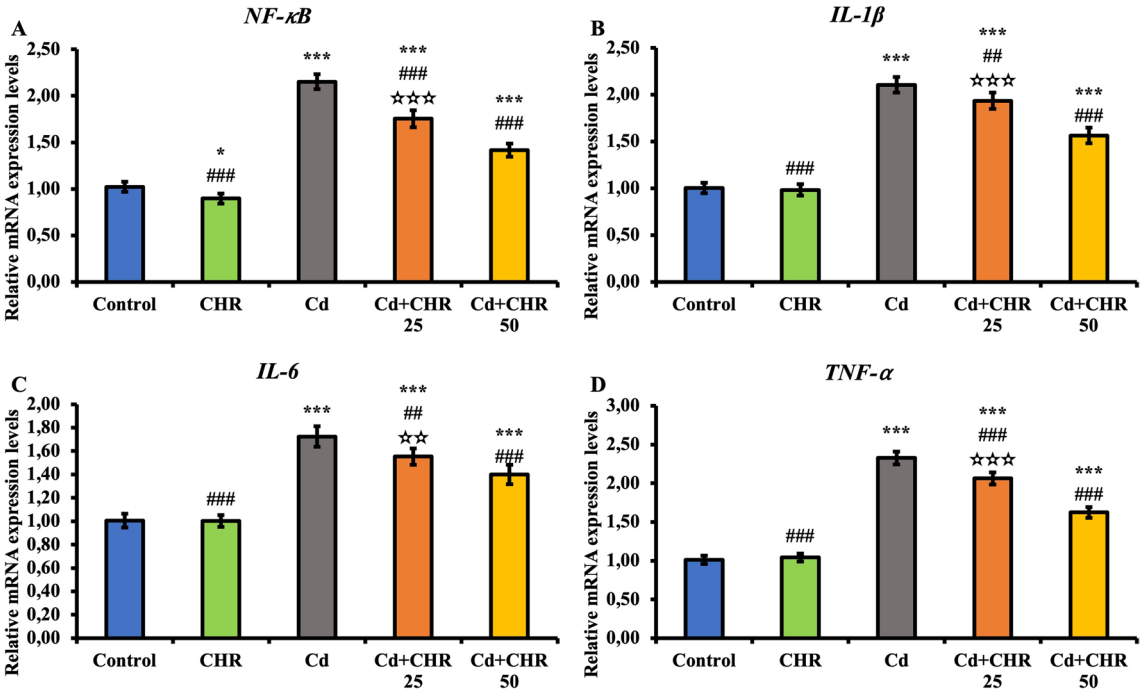

Fig. 3 Effects of Cd and CHR administrations on NF-κB, IL-1β, IL-6 and TNF-α activities in lung tissue of rats. NF-κB: Nuclear factor kappa-B, IL-1β: Interleukin-1 beta, IL-6: Interleukin-6, TNF-α: Tumor necrosis factor alpha. Statistical significance (Control vs others: * $P < 0.05$, ** $p < 0.01$, *** $p < 0.001$, Cd vs others: $^{\#}P < 0.05$, $^{\#\#}p < 0.01$, $^{\#\#\#}p < 0.001$, Cd + CHR 25 vs Cd + CHR 50: $^{\star}P < 0.05$, $^{\star\star}p < 0.01$, $^{\star\star\star}p < 0.001$) was analyzed using One Way ANOVA

CHR administration increased Cd-induced decreased expression of Bcl-2 (low dose; 1.58-fold, high dose; 1.78-fold), an antiapoptotic gene, while suppressing Bax (low dose; 1.11-fold, high dose; 1.33-fold) and Caspase-3 (low dose; 1.28-fold, high dose; 1.39-fold) expression.

H&E Findings

The effects of CHR on Cd-induced morphologic changes are given in Fig. 7 Top row. When the lung tissues of the control and CHR groups were examined, the parenchyma was normal and the architecture of the alveoli, alveolar sacs and bronchioles were good. Type 1 and type 2 pneumocytes were selectable and smooth. CHR administration also did not cause any structural changes in the lung. Especially diffuse pulmonary hemorrhage (red arrow) was quite high as a result of Cd administration. Inflammatory cell infiltration (yellow arrow) was also observed in the lung tissues of this group. In addition, thickening of the alveolar wall (black arrow), rupture of

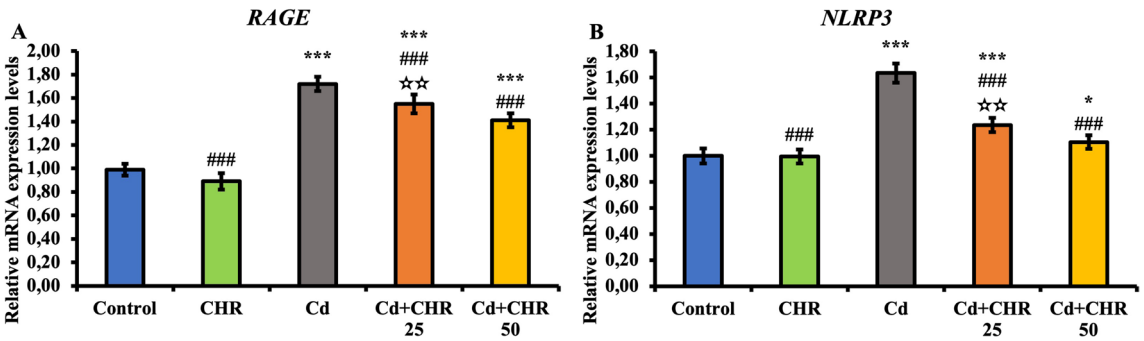

Fig. 4 RAGE and NRLP3 protein levels in lung tissues of rats after Cd and CHR administrations. RAGE: Receptor for advanced glycation end products, NRLP3: NOD-like receptor family, pyrin domain containing 3. Statistical significance (Control vs others: * $P < 0.05$, ** $p < 0.01$, *** $p < 0.001$, Cd vs others: $^{\#}P < 0.05$, $^{\#\#}p < 0.01$, $^{\#\#\#}p < 0.001$, Cd + CHR 25 vs Cd + CHR 50: $^{\star}P < 0.05$, $^{\star\star}p < 0.01$, $^{\star\star\star}p < 0.001$) was analyzed using One Way ANOVA

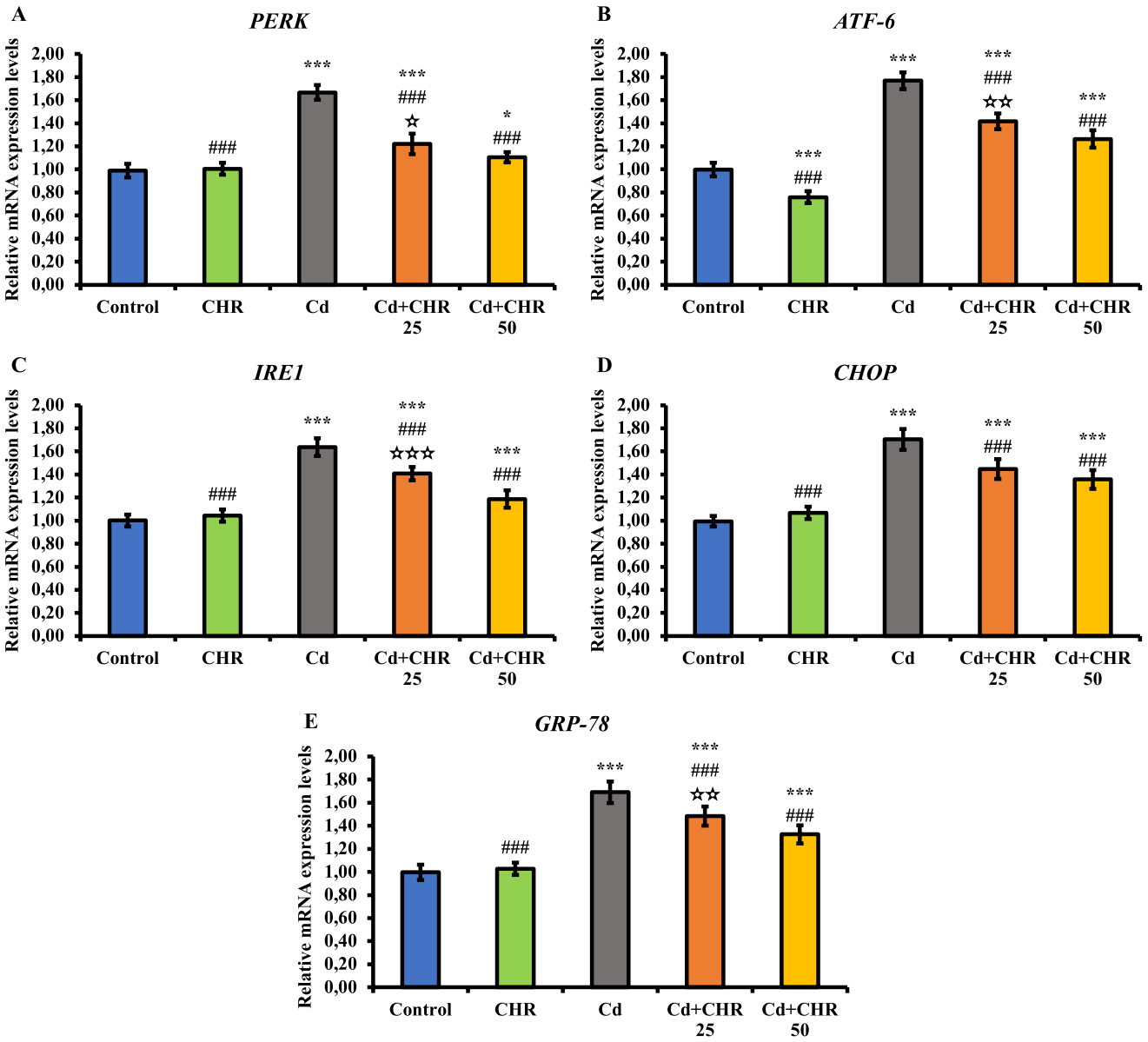

Fig. 5 Effects of Cd and CHR administrations on PERK, ATF-6, IRE1, CHOP and GRP-78 activities in lung tissue of rats. PERK: Protein kinase RNA-like ER kinase, ATF-6: Activating transcription factor 6, IRE1: Inositol-requiring enzyme 1, CHOP: C/EBP homologous protein, GRP-78: Glucose-regulated protein 78. Statistical significance (Control vs others: * $P < 0.05$, ** $p < 0.01$, *** $p < 0.001$, Cd vs others: $^{\#}$ $P < 0.05$, $^{\#\#}$ $p < 0.01$, $^{\#\#\#}$ $p < 0.001$, Cd + CHR 25 vs Cd + CHR 50: $^{\star}P < 0.05$, ** $p < 0.01$, *** $p < 0.001$) was analyzed using One Way ANOVA

bronchiole walls and desquamation of alveolar wall cells were remarkable. Collagen deposition was observed in some areas of Cd-induced lung tissues. As a result of CHR administration together with Cd, lung parenchyma was mostly normal in both dose groups. Hemorrhages were observed in rare areas.

Masson Trichrome Findings

The effects of CHR on Cd-induced morphologic changes are given in Fig. 7 Bottom row. In the sections stained with Masson's trichrome, a significant decrease was observed in Cd-induced increased interalveolar septa, peri-vascular spaces and peri-bronchial collagen fibers (blue arrow) with the application of CHR.

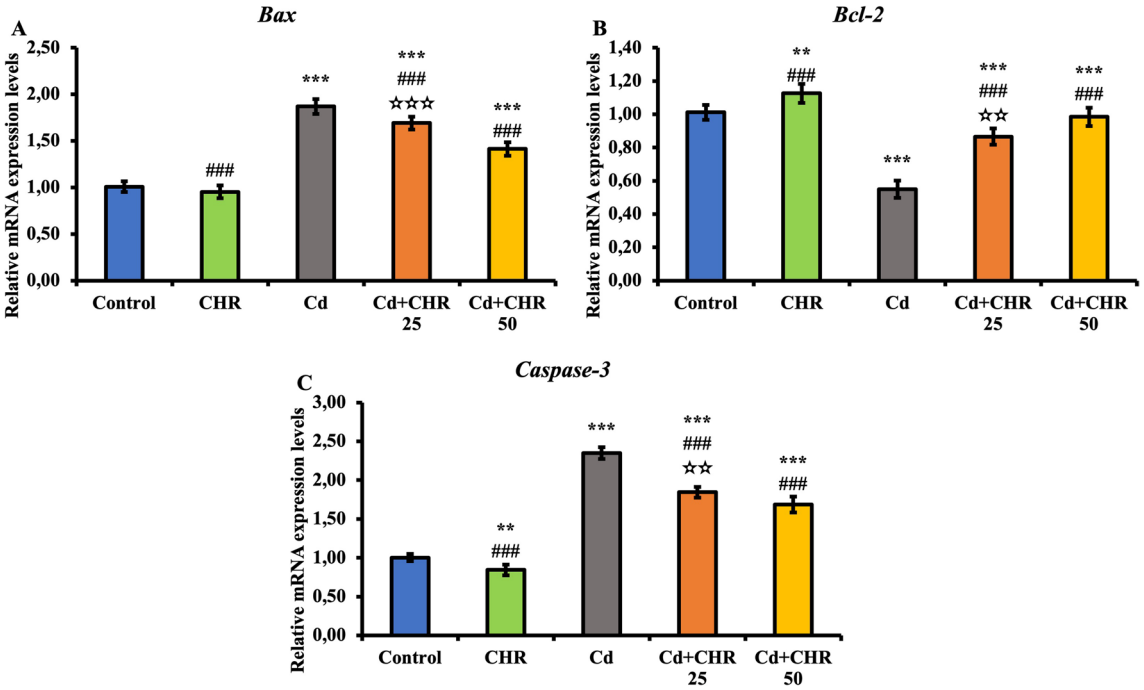

Fig. 6 Effects of Cd and CHR administrations on Bax, Bcl-2 and Caspase-3 activities in lung tissue of rats. Bax: Bcl-2-associated x protein, Bcl-2: B-cell lymphoma-2, Caspase-3: Cysteine aspartate-specific protease-3. Statistical significance (Control vs others: * $P < 0.05$, ** $p < 0.01$, *** $p < 0.001$, Cd vs others: $^{\#}P < 0.05$, $^{\#\#}p < 0.01$, $^{\#\#\#}p < 0.001$, Cd + CHR 25 vs Cd + CHR 50: $^{\star}P < 0.05$, $^{\star\star}p < 0.01$, $^{\star\star\star}p < 0.001$) was analyzed using One Way ANOVA

Effects of Cd and CHR administration on immunohistochemical changes in lung tissue

NF-κB, an inflammation marker, is given in the top row in Fig. 8, and Caspase-3, an apoptosis marker, in Fig. 8, in the bottom row. As a result of NF-κB staining, positivity in alveolar wall cells was rarely detected in control (% 15.56) and CHR (% 14.46) groups. Following NF-κB staining, there was a statistically significant increase in immunopositivity in the Cd group (%66.84) compared to the other groups ($p < 0.001$). NF-κB immunopositivity decreased significantly in all groups treated with CHR after Cd ($p < 0.001$). Especially 50 mg/kg CHR (%27.92) administration was more effective than other

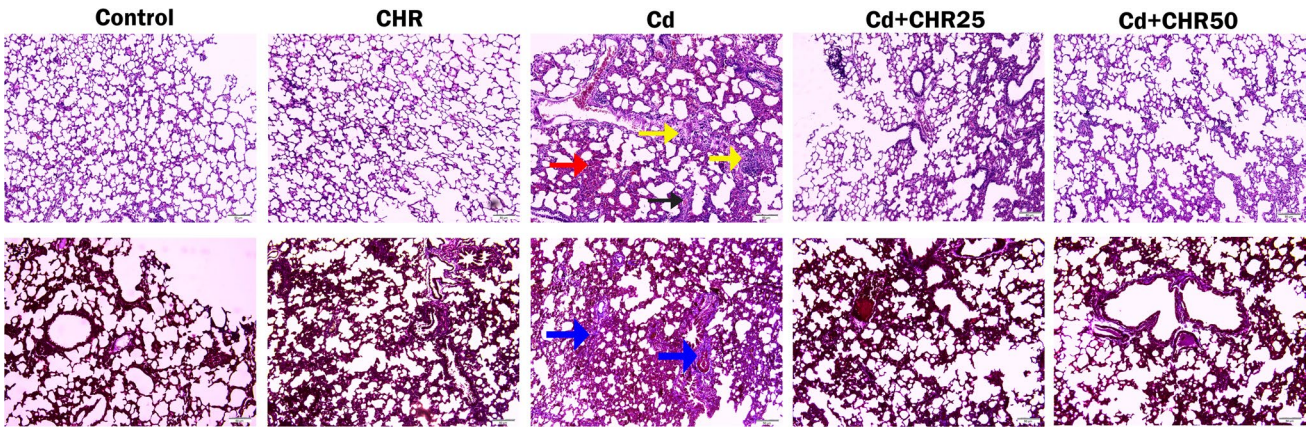

Fig. 7 Photomicrographs of histological changes in lung tissue. (Top row:H&E staining, Bottom row: Masson Trichrome, 200x). Control group, CHR (Chrysin) group, Cd (Cadmium) group; yellow arrow: inflammatory cell infiltration, red arrow: bleeding, black arrow: alveolar wall thickening, blue arrow: indicates high deposition of collagen fibers (blue color indicates collagen), Cd + CHR 25 (Cadmium + Chrysin 25) group; Cd + CHR 50 (Cadmium + Chrysin 50) group

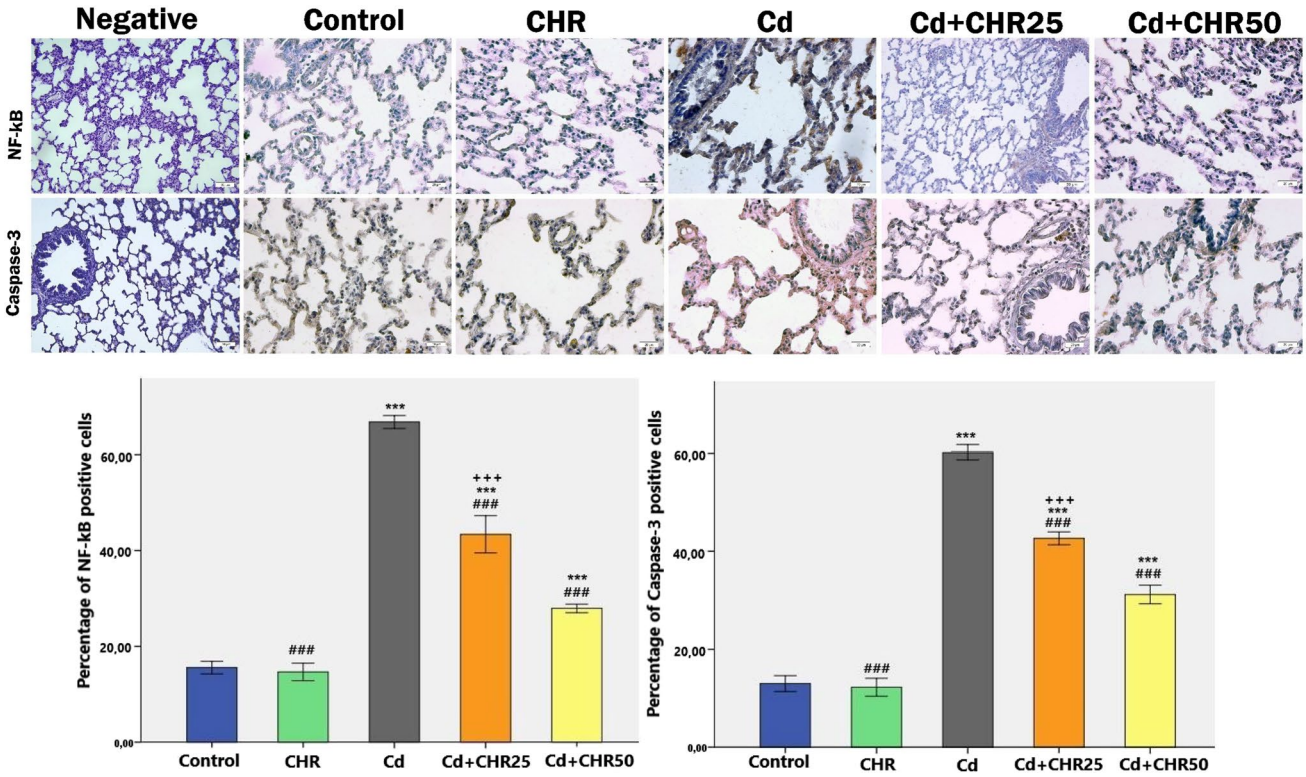

Fig. 8 NF-κB and Caspase-3 immunohistochemical staining. (Top row: NF-kB, Bottom row: Caspase 3, 200x). Control group, Control group, CHR (Chrysin) group, Cd (Cadmium) group, Cd + CHR 25 (Cadmium + Chrysin 25) group; Cd + CHR 50 (Cadmium + Chrysin 50) group. NF-κB and Caspase-3 positive cell percentage score. Statistical significance (Control vs others: * $P < 0.05$, ** $p < 0.01$, *** $p < 0.001$, Cd vs others: $^{\#}P < 0.05$, $^{\#\#}p < 0.01$, $^{\#\#\#}p < 0.001$, Cd + CHR 25 vs Cd + CHR 50: $^{+}P < 0.05$, $^{++}p < 0.01$, $^{+++}p < 0.001$) was analyzed using One Way ANOVA

doses ($p < 0.001$). Apoptosis was significantly increased in the Cd-administered group (%60.15) compared to the other groups ($p < 0.001$). Caspase-3 immunoreactivity showed weak immunostaining in alveolar cells in control (%12.98) and CHR (%12.24) groups. In addition, it was found that CHR (%42.66, 31.18) administration with Cd decreased immunoreactivity ($p < 0.001$).

Discussion

Cd, one of the most toxic metals in the environment, poses a risk to living things due to its ease of dissolution and decomposition (Dong et al. 2022). There is mounting evidence that one of the primary target organs for cadmium exposure is the lung, which is impacted by this toxicity (Dashtbanei & Keshtmand 2022, El-Ebiary et al. 2016). To mitigate the pulmonary toxicity caused by cadmium exposure, various antioxidant treatments have been tested in earlier studies (El-Ebiary et al. 2016; Yesildag et al. 2022). This study represents the first approach using CHR for the treatment of Cd toxicity in the lungs. Thus, this study was conducted to investigate the potential protective effect of CHR on Cd-induced changes in lung function and morphology. Degenerative effects of Cd toxicity on the lung are well-known, however, its pathophysiology is still largely unknown. Many cellular damage mechanisms play a role in metal toxicity (Akaras et al. 2023; Gur et al. 2023; Khanna et al. 2016; Paithankar et al. 2021).

Oxidative stress is the primary mechanism by which Cd exposure mediates lung injury (Yesildag et al. 2022). Cd disturbs the balance of the redox system in the cell and increases lipid peroxidation (Wang et al. 2019; Zhang et al. 2022a). One of the key markers of oxidative stress is MDA, which is the end product of lipid peroxidation (Varışlı et al. 2022). The current study demonstrated that MDA levels were raised by Cd treatment. The oxidation of fatty acid double bonds in phospholipids is thought to be the cause of the biochemical alterations that occur after exposure to Cd. This oxidation is likely to increase oxidative stress because it increases the fluidity and permeability of cell membranes (Zhu et al. 2019). In the present study, CHR treatment decreased MDA levels and provided protection against Cd-induced lipid peroxidation.

Cd, on the one hand, triggers an increase in ROS and, leads to a disruption in the balance between oxidants and antioxidants on the other (Dashtbanei & Keshtmand 2022; Cui et al. 2023). Enzymatic (SOD, CAT, GPx) and non-enzymatic (GSH) antioxidant defense systems maintain the control of cellular redox balance in the body under normal conditions. SOD is involved in the conversion of superoxide anion radical into H_2O_2 and CAT and GPx are involved in the decomposition of H_2O_2 into H_2O and O_2 (Akaras et al. 2023; Wang et al. 2023a, b). Glutathione, which is abundant in cells, plays a crucial role in Cd-induced oxidative stress by directly reacting with electrofilms or as a cofactor. (for GPx and Glutathione Transferase (GST) enzymes) (Boldrini et al. 2022; Turk et al. 2019). GSH also modulates the redox state of specific thiol residues of Cd-targeted proteins such as caspases, stress kinases and transcriptional factors (Turk et al. 2019). In the present study, Cd was shown to inhibit SOD, CAT and GPx activities and decrease GSH stores in lung tissues. Probably Cd disturbs the redox balance by removing cations from the active sites of antioxidant enzymes. It is also presumed to inhibit proteins, including antioxidant enzymes, by binding to their sulfhydryl groups. Also, heavy metals disturb the oxidant-antioxidant balance by causing the accumulation of ROS through the degradation of cellular GSH (Gur et al. 2023; Yesildag et al. 2022). Our study showed that CHR treatment with Cd increased SOD, CAT, GPx activities and GSH levels in a dose-dependent manner and decreased Cd-induced oxidative damage. Previous studies reported that CHR showed antioxidant properties and reduced oxidative stress in different toxicity models (Khezri et al. 2020; Soliman et al. 2022). In addition, in a study conducted by Kandemir et al. it was emphasized that CHR improved antioxidant capacity (Kandemir et al. 2017). It has been observed that due to the antioxidant properties of the hydroxyl groups in the structure of CHR, it reduces lipid peroxidation in lung tissue, increases enzymatic and non-enzymatic markers, and preserves membrane integrity.

The inflammation process triggered by oxidative stress is one of the important mechanisms that contribute to the progression of Cd-induced lung injury (Antar et al. 2022). Increased ROS also increases inflammation by triggering NF-κB expression along with oxidative stress (Küçükler et al. 2021). NF-κB factor, the main signaling pathway of the inflammatory process, plays a crucial role in stimulating inflammation and immune response in response to various factors including IL-1β, IL-6 and TNF-α (Yardım et al. 2021). Also, the NF-κB is a transcription factor involved in the expression of various genes including cell cycle, growth factors, adhesion molecules, and antiapoptotic factors (Gur et al. 2022a; Turk et al. 2019). Previous studies have been reported that Cd damages different tissues by triggering inflammation (Bakr et al. 2022; El-Ebiary et al. 2016). In the present study, it was found that Cd increased the expression of the NF-κB gene as a result of increased ROS accumulation, which in turn increased the levels of IL-1β, IL-6, and TNF-α transcripts. On the other hand, it was ascertained that CHR scavenges ROS thanks to its antioxidant properties and thus protects the lung tissue against inflammation by preventing the activation of proinflammatory genes. Possibly O-methylation of chrysin significantly improved lung antiinflammatory properties through more pronounced inhibition of the NF-kB signaling pathway. Kandemir et al. revealed that CHR's antiinflammatory property is the reason why NF-κB, TNF-α and IL-1β levels dropped in an experimental animal study (Kandemir et al. 2017).

Another pathway involved in the regulation of cell proliferation, cell regeneration, oxidative stress, apoptosis, immune response and inflammation via NF-κB is the receptor for advanced glycation end products (RAGE) (Sun et al. 2021). RAGE is a multiligand member of the immunoglobulin protein superfamily that binds multiple ligands and is abundantly expressed in the lung. Increasing evidence suggests that RAGE is involved in the pathogenesis of various pulmonary disorders (Downs et al. 2018; Lenga Ma Bonda et al. 2022). In the current study, RAGE expression was found to be increased in the Cd-treated group compared to the control group. Our results demonstrated that the beneficial effect of CHR against Cd injury due to its antiinflammatory effect and inactivation of the inflammation mechanism. In other words, CHR treatment significantly reduced RAGE expression and deactivated the onset of inflammation.

It is known that during inflammation, the RAGE signaling pathway, which stimulates the NF-κB's downstream signaling pathway, increases the production of NLRP3. NLRP3 is a critical component of the innate immune system that responds to stressors and intracellular infections. NLRP3 is a multiprotein immune sensor complex consisting of three subunits: NLRP3, adaptor subunit (ASC) and pro-caspase-1 subunit (Eisa et al. 2021; Sun et al. 2021). Studies have established that Advanced glycation end products (AGEs) can induce NLRP3 inflammasome activation in inflammation process (Oh et al. 2021; Yu et al. 2018). Although the precise mechanism underlying AGE-induced activation of NF-κB and NLRP3 has not yet been fully elucidated, activation may be directly caused by the perception of cellular stress signals, particularly ROS overproduction or RAGE overexpression (Yu et al. 2018). Also, NLRP3 may be a promising drug target regulating lung inflammation and inhibiting the immunopathology of pulmonary diseases in particular, thus attracting close attention of clinical and experimental research (Jin et al. 2021; Lenga Ma Bonda et al. 2022; Luo et al. 2021). The ability of cadmium to induce NLRP3 activation has been previously demonstrated (Li et al. 2021). In the present study, our results showed that Cd increased NLRP3 protein

expression levels. In addition, NLRP3 protein expression levels decreased with CHR treatment. The combined data of the present study revealed that CHR can regulate the inflammatory response by inhibiting NLRP3 and NF-κB signaling pathway, thereby mitigating Cd toxicity.

Oxidative damage also affects cell death pathways (Dai et al. 2022). Evidences suggest that one of the mechanisms triggered by oxidative stress is endoplasmic reticulum stress (Caglayan et al. 2022, Gur & Kandemir 2023, Gur et al. 2022b). The endoplasmic reticulum is a vital organelle that is involved in protein synthesis, folding and maturation, and calcium homeostasis. Environmental and physiological factors contribute to the accumulation of unfolded and misfolded proteins in the ER lumen, as well as Ca imbalance (Varışlı et al. 2023). As a result of this, cells develop an unfolded protein response (UPR). As the stress persists, the UPR continues to elongate, ER stress develops, and the cell undergoes apoptosis. UPR transduction is mediated by ER transmembrane sensors including PERK, ATF-6, and IRE1. These sensors mostly bind to and dissociate from GRP78, an essential ER chaperone. GRP78 is overexpressed in case of ER stress. CHOP is another important ER indicator. Another important indicator of ER stress is CHOP, which is an important factor involved in apoptosis (Ileriturk et al. 2023, 2022; Kandemir et al. 2022; Varışlı et al. 2023). Although UPR plays an important role in the pathogenesis of pulmonary diseases, it has been reported that ER stress is triggered in heavy metal-induced pulmonary toxicity (Mahalanobish et al. 2019; Wang et al. 2023a, b). The current study showed that Cd exposure up-regulated PERK, ATF-6, IRE1, CHOP, and GRP78 genes and triggered ER stress. At the same time, CHR treatment was found to suppress the expression of PERK, ATF-6, IRE1, CHOP and GRP78 genes. This study revealed that oxidative stress and mitochondrial dysfunction may be the underlying mechanism of ER stress in addition to heavy metal load.

Increased ER stress reduces the mitochondrial membrane potential by disturbing calcium balance if not eliminated. Mitochondria, the power centre of the cell, are an integral component of many cell signaling cascades (Wen et al. 2022; Zhang et al. 2022c; Lin et al. 2023). Previous studies on Cd toxicity have identified mitochondria as a target organelle (Cao et al. 2021, Dashtbanei & Keshtmand 2022, Yesildag et al. 2022). The function of lung cells is highly reliant on the functionality of mitochondrial membrane integrity. As a result, one of the most important goals is to repair mitochondrial damage in pulmonary function integrity. If the damage is not repaired, the balance between antiapoptotic Bcl-2 and proapoptotic Bax, which protects the mitochondrial membrane's integrity, is disturbed, and cells undergo apoptosis (Küçükler et al. 2022; Yesildag et al. 2022, Zhang et. 2022b). Bcl-2 promotes the release of cytochrome C (Cyt C) into the cytoplasm by increasing the permeability of the mitochondrial membrane and triggers Caspase-3 (Lei et al. 2023). A previous study reported that Cd administration increased Caspase-3 and Bax levels in rats and decreased Bcl-2 levels by triggering the apoptotic process (Yesildag et al. 2022). In a study with Chrisin, caspase 3 was evaluated immunohistochemically and it was observed that CHR administration reduced caspase 3 immunoreactivity compared to the toxic group (El-Marasy et al. 2019). In the present study, it was found that ROS increased as a result of Cd administration disrupted mitochondrial membrane integrity and accordingly increased Bax and Caspase-3 protein expression compared to the control. However, it was observed that Bcl-2 expression was lower in the lung tissues in the Cd group compared to the control group and this increased apoptosis. CHR supplementation with Cd inhibited the Bax/Bcl-2/Caspase-3 pathway by blocking ER stress-induced cytochrome C release and thus modulated the apoptosis process. This protective effect of CHR is hypothesized to be due to its inhibition of ER stress induced by oxidative stress and attenuation of apoptosis. In line with this view, antiapoptotic effects have been identified in different toxicity studies on CHR (Küçükler et al. 2022; Varışlı et al. 2023).

The lungs of rats exposed to cadmium toxicity showed structural changes such as occluded capillaries and diffuse pulmonary hemorrhage, thickened alveolar walls, increased collagen, interstitial edema, and inflammatory cell infiltration in the current study. These findings suggest that Cd has a significant detrimental effect on lung parenchyma. Our results demonstrated lung benefits comparable to those obtained with intratracheal, inhalation, and intrathoracic Cd administration (El-Ebiary et al. 2016; Oh et al. 2014). This could be explained by increased permeability of pulmonary epithelial cells and severe haemorrhages in the lungs caused by Cd exposure disrupting the functioning of the air-blood barrier. Other studies reporting structural changes in the lungs of Cd-exposed rats supported these findings (El-Ebiary et al. 2016; Naidoo et al. 2019). The accumulation of Cd in the tissue, which causes pathological changes and is a highly toxic metal, may be the cause of these findings. When compared to the Cd group, lung histological examination showed that bronchioles were normal and bleeding was limited in the Cd + CHR group. Furthermore, CHR administration reduced the alveolar wall thickness compared to the Cd treated group. CHR's antioxidant and antiinflammatory properties have been reported in previous studies to protect connective tissue and cell structures in various tissues from some attacks (Kseibati et al. 2020; Soliman et al. 2022).

Conclusion

Given the increasing incidence and prevalence of Cd toxicity, it is important to find the most effective and safe treatment method or combination. The ameliorative effects of CHR against Cd-induced toxicity were demonstrated in this study, which characterized by lung histopathological changes as well as increased oxidative stress, inflammation, ER stress, and apoptosis. Taking all of this information into account, it was concluded that CHR supportive therapy in conjunction with Cd may be useful in alleviating or ameliorating Cd-induced lung toxicity.

Author contributions All authors contributed to the study conception and design. Material preparation, data collection and analysis were performed by [Nurhan Akaras], [Mustafa Ileriturk], [Cihan Gur], [Sefa Kucukler], [Mehmet Oz] and [Fatih Mehmet Kandemir]. The first draft of the manuscript was written by [Nurhan Akaras] and [Cihan Gur] and all authors commented on previous versions of the manuscript. All authors read and approved the final manuscript.

Funding Not applicable.

Data availability All relevant data are within the paper.

Declarations

Ethics approval The study was approved by Necmettin Erbakan University Animal Experiments Local Ethics Committee (no. 2022–55).

Consent to participate Not applicable.

Consent for publication Not applicable.

Conflict of interest The authors declare that there is no conflict of interest.

References

Aebi H (1984): [13] Catalase in vitro, Methods in enzymology. Elsevier, pp. 121–126

Akaras N, Gur C, Kucukler S, Kandemir FM (2023) Zingerone reduces sodium arsenite-induced nephrotoxicity by regulating oxidative stress, inflammation, apoptosis and histopathological changes. Chem Biol Interact 374:110410

Aksu EH, Kandemir FM, Küçükler S, Mahamadu A (2018) Improvement in colistin-induced reproductive damage, apoptosis, and autophagy in testes via reducing oxidative stress by chrysin. J Biochem Mol Toxicol 32:e22201

Antar SA, El-Gammal MA, Hazem RM, Moustafa YM (2022) Etanercept Mitigates Cadmium Chloride-induced Testicular Damage in Rats" An Insight into Autophagy, Apoptosis, Oxidative Stress and Inflammation". Environ Sci Pollut Res 29:28194–28207

Arafa MH, Mohamed DA, Atteia HH (2015) Ameliorative effect of N-acetyl cysteine on alpha-cypermethrin-induced pulmonary toxicity in male rats. Environ Toxicol 30:26–43

Bakr AG, Hassanein EH, Ali FE, El-Shoura EA (2022) Combined apocynin and carvedilol protect against cadmium-induced testicular damage via modulation of inflammatory response and redox-sensitive pathways. Life Sci 311:121152

Boldrini GG, Martin Molinero G, Perez Chaca MV, Ciminari ME, Moyano F, Córdoba ME, Pennacchio G, Fanelli M, Álvarez SM, Gómez NN (2022) Glycine max (soy) based diet improves antioxidant defenses and prevents cell death in cadmium intoxicated lungs. Biometals 35:229–244

Caglayan C, Kandemir FM, Ayna A, Gür C, Küçükler S, Darendelioğlu E (2022) Neuroprotective effects of 18β-glycyrrhetinic acid against bisphenol A-induced neurotoxicity in rats: involvement of neuronal apoptosis, endoplasmic reticulum stress and JAK1/STAT1 signaling pathway. Metab Brain Dis 37:1931–1940

Cao X, Fu M, Bi R, Zheng X, Fu B, Tian S, Liu C, Li Q, Liu J (2021) Cadmium induced BEAS-2B cells apoptosis and mitochondria damage via MAPK signaling pathway. Chemosphere 263:128346

Cao P, Nie G, Luo J, Hu R, Li G, Hu G, Zhang C (2022) Cadmium and molybdenum co-induce pyroptosis and apoptosis via the PTEN/PI3K/AKT axis in the livers of Shaoxing ducks (Anas platyrhynchos). Food Funct 13(4):2142–2154

Cui Y, Li Z, Xiao Q, Ge J, Jiang W, Wang X, Wang Z, Yuan Y, Zhuang Y, Hao W, Jiang J, Meng Q, Wei X (2023) 1,4-Naphthoquinone-coated black carbon nanoparticles up-regulation POR/FTL/IL-33 axis in THP1 cells. Ecotoxicol Environ Saf 249:114381

Dai XY, Zhu SY, Chen J, Li MZ, Zhao Y, Talukder M, Li JL (2022) Lycopene alleviates di(2-ethylhexyl) phthalate-induced splenic injury by activating P62-Keap1-NRF2 signaling. Food and Chemical Toxicology : an International Journal Published for the British Industrial Biological Research Association 168:113324

Dashtbanei S, Keshtmand Z (2022) A Mixture of Multi-Strain Probiotics (Lactobacillus rhamnosus, Lactobacillus helveticus, and Lactobacillus casei) had Anti-Inflammatory, Anti-Apoptotic, and Anti-Oxidative Effects in Oxidative Injuries Induced By Cadmium in Small Intestine and Lung. Probiotics and Antimicrobial Proteins, pp 1–13

Dong W, Yan L, Tan Y, Chen S, Zhang K, Gong Z, Liu W, Zou H, Song R, Zhu J (2022) Melatonin improves mitochondrial function by preventing mitochondrial fission in cadmium-induced rat proximal tubular cell injury via SIRT1–PGC-1α pathway activation. Ecotoxicol Environ Saf 242:113879

Downs CA, Johnson NM, Tsaprailis G, Helms MN (2018) RAGE-induced changes in the proteome of alveolar epithelial cells. J Proteomics 177:11–20

Eisa NH, Khodir AE, El-Sherbiny M, Elsherbiny NM, Said E (2021) Phenethyl isothiocyanate attenuates diabetic nephropathy via modulation of glycative/oxidative/inflammatory signaling in diabetic rats. Biomed Pharmacother 142:111666

El-Ebiary AA, El-Ghaiesh S, Hantash E, Alomar S (2016) Mitigation of cadmium-induced lung injury by Nigella sativa oil. Environ Sci Pollut Res 23:25356–25363

Elkin ER, Higgins C, Aung MT, Bakulski KM (2022) Metals Exposures and DNA Methylation: Current Evidence and Future Directions. Current Environmental Health Reports, pp 1–24

El-Marasy SA, El Awdan SA, Abd-Elsalam RM (2019) Protective role of chrysin on thioacetamide-induced hepatic encephalopathy in rats. Chem Biol Interact 299:111–119

Gao Y, Xu Y, Wu D, Yu F, Yang L, Yao Y, Liang Z, Lau AT (2017) Progressive silencing of the zinc transporter Zip8 (Slc39a8) in chronic cadmium-exposed lung epithelial cells. Acta Biochimica et Biophysica Sinica

Genchi G, Sinicropi MS, Lauria G, Carocci A, Catalano A (2020) The Effects of Cadmium Toxicity. Int J Environ Res Public Health 17:3782

Guo H, Hu R, Huang G, Pu W, Chu X, Xing C, Zhang C (2022) Molybdenum and cadmium co-exposure induces endoplasmic reticulum stress-mediated apoptosis by Th1 polarization in Shaoxing duck (Anas platyrhyncha) spleens. Chemosphere 298:134275

Gur C, Kandemir FM (2023) Molecular and biochemical investigation of the protective effects of rutin against liver and kidney toxicity caused by malathion administration in a rat model. Environ Toxicol 38:555–565

Gur C, Kandemir FM, Caglayan C, Satıcı E (2022a) Chemopreventive effects of hesperidin against paclitaxel-induced hepatotoxicity and nephrotoxicity via amendment of Nrf2/HO-1 and caspase-3/Bax/Bcl-2 signaling pathways. Chem Biol Interact 365:110073

Gur C, Kandemir O, Kandemir FM (2022b) Investigation of the effects of hesperidin administration on abamectin-induced testicular toxicity in rats through oxidative stress, endoplasmic reticulum stress, inflammation, apoptosis, autophagy, and JAK2/STAT3 pathways. Environ Toxicol 37:401–412

Gur C, Akarsu SA, Akaras N, Tuncer SC, Kandemir FM (2023) Carvacrol reduces abnormal and dead sperm counts by attenuating sodium arsenite-induced oxidative stress, inflammation, apoptosis, and autophagy in the testicular tissues of rats. Environ Toxicol

Hanedan B, Ozkaraca M, Kirbas A, Kandemir FM, Aktas MS, Kilic K, Comakli S, Kucukler S, Bilgili A (2018) Investigation of the effects of hesperidin and chrysin on renal injury induced by colistin in rats. Biomed Pharmacother 108:1607–1616

Ileriturk M, Benzer F, Aksu EH, Yildirim S, Kandemir FM, Dogan T, Dortbudak MB, Genc A (2021) Chrysin protects against testicular toxicity caused by lead acetate in rats with its antioxidant, anti-inflammatory, and antiapoptotic properties. J Food Biochem 45:e13593

Ileriturk M, Kandemir O, Kandemir FM (2022) Evaluation of protective effects of quercetin against cypermethrin-induced lung toxicity in rats via oxidative stress, inflammation, apoptosis, autophagy, and endoplasmic reticulum stress pathway. Environ Toxicol 37:2639–2650

Ileriturk M, Kandemir O, Akaras N, Simsek H, Genc A, Kandemir FM (2023) Hesperidin has a Protective Effect on Paclitaxel-induced Testicular Toxicity through Regulating Oxidative Stress, Apoptosis, Inflammation and Endoplasmic Reticulum Stress. Reproductive Toxicology, p 108369

Järup L (2003) Hazards of heavy metal contamination. Br Med Bull 68:167–182

Jin S, Ding X, Yang C, Li W, Deng M, Liao H, Lv X, Pitt BR, Billiar TR, Zhang L-M (2021) Mechanical ventilation exacerbates poly (I: C) induced acute lung injury: Central role for caspase-11 and gut-lung axis. Front Immunol 12:693874

Kandemir FM, Kucukler S, Eldutar E, Caglayan C, Gülçin İ (2017) Chrysin protects rat kidney from paracetamol-induced oxidative stress, inflammation, apoptosis, and autophagy: a multi-biomarker approach. Sci Pharm 85:4

Kandemir FM, Caglayan C, Darendelioğlu E, Küçükler S, İzol E, Kandemir Ö (2021) Modulatory effects of carvacrol against cadmium-induced hepatotoxicity and nephrotoxicity by molecular targeting regulation. Life Sci 277:119610

Kandemir FM, Ileriturk M, Gur C (2022) Rutin protects rat liver and kidney from sodium valproate-induce damage by attenuating oxidative stress, ER stress, inflammation, apoptosis and autophagy. Mol Biol Rep 49:6063–6074

Kassab AA, Aboregela AM, Shalaby AM (2020) Edaravone attenuates lung injury in a hind limb ischemia-reperfusion rat model: A histological, immunohistochemical and biochemical study. Annals of Anatomy-Anatomischer Anzeiger 228:151433

Khanna S, Mitra S, Lakhera PC, Khandelwal S (2016) N-acetylcysteine effectively mitigates cadmium-induced oxidative damage and cell death in Leydig cells in vitro. Drug Chem Toxicol 39:74–80

Khezri S, Sabzalipour T, Jahedsani A, Azizian S, Atashbar S, Salimi A (2020) Chrysin ameliorates aluminum p hosphide-induced oxidative stress and mitochondrial damages in rat cardiomyocytes and isolated mitochondria. Environ Toxicol 35:1114–1124

Kseibati MO, Sharawy MH, Salem HA (2020) Chrysin mitigates bleomycin-induced pulmonary fibrosis in rats through regulating inflammation, oxidative stress, and hypoxia. Int Immunopharmacol 89:107011

Kucukler S, Benzer F, Yildirim S, Gur C, Kandemir FM, Bengu AS, Ayna A, Caglayan C, Dortbudak MB (2021) Protective effects of chrysin against oxidative stress and inflammation induced by lead acetate in rat kidneys: a biochemical and histopathological approach. Biol Trace Elem Res 199:1501–1514

Küçükler S, Kandemir FM, Yıldırım S (2022) Protective effect of chrysin on indomethacin induced gastric ulcer in rats: role of multi-pathway regulation. Biotech Histochem 97:490–503

Kulas J, Tucovic D, Zeljkovic M, Popovic D, Aleksandrov AP, Kataranovski M, Mirkov I (2021) Aryl hydrocarbon receptor is involved in the proinflammatory cytokine response to cadmium. Biomed Environ Sci 34:192–202

Lawrence RA, Burk RF (1976) Glutathione peroxidase activity in selenium-deficient rat liver. Biochem Biophys Res Commun 71:952–958

Lei Y, Zhang W, Gao M, Lin H (2023) Mechanism of evodiamine blocking Nrf2/MAPK pathway to inhibit apoptosis of grass carp hepatocytes induced by DEHP. Comparative biochemistry and physiology. Toxicology & Pharmacology CBP 263:109506

Lenga Ma Bonda W, Fournet M, Zhai R, Lutz J, Blondonnet R, Bourgne C, Leclaire C, Saint-Béat C, Theilliere C, Belville C (2022) Receptor for Advanced Glycation End-Products Promotes Activation of Alveolar Macrophages through the NLRP3 Inflammasome/TXNIP Axis in Acute Lung Injury. Int J Mol Sci 23:11659

Li Z, Chi H, Zhu W, Yang G, Song J, Mo L, Zhang Y, Deng Y, Xu F, Yang J (2021) Cadmium induces renal inflammation by activating the NLRP3 inflammasome through ROS/MAPK/NF-κB pathway in vitro and in vivo. Arch Toxicol 95:3497–3513

Lin S, Yang F, Hu M, Chen J, Chen G, Hu A, Li X, Fu D, Xing C, Xiong Z, Wu Y, Cao H (2023) Selenium alleviates cadmium-induced mitophagy through FUNDC1-mediated mitochondrial quality control pathway in the lungs of sheep. Environ Pollut 319:120954

Liu X, Ma C, Wang X, Wang W, Li Z, Wang X, Wang P, Sun W, Xue B (2017) Hydrogen coadministration slows the development of COPD-like lung disease in a cigarette smoke-induced rat model. Int J Chron Obstruct Pulmon Dis 12:1309–1324

Livak KJ, Schmittgen TD (2001) Analysis of relative gene expression data using real-time quantitative PCR and the 2− ΔΔCT method. Methods 25:402–408

Lowry OH, Rosebrough NJ, Farr AL, Randall RJ (1951) Protein measurement with the Folin phenol reagent. J Biol Chem 193:265–275

Luo D, Dai W, Feng X, Ding C, Shao Q, Xiao R, Zhao N, Peng W, Yang Y, Cui Y (2021) Suppression of lncRNA NLRP3 inhibits NLRP3-triggered inflammatory responses in early acute lung injury. Cell Death Dis 12:898

Mahalanobish S, Saha S, Dutta S, Sil PC (2019) Mangiferin alleviates arsenic induced oxidative lung injury via upregulation of the Nrf2-HO1 axis. Food Chem Toxicol 126:41–55

Naidoo SVK, Bester MJ, Arbi S, Venter C, Dhanraj P, Oberholzer HM (2019) Oral exposure to cadmium and mercury alone and in

combination causes damage to the lung tissue of Sprague-Dawley rats. Environ Toxicol Pharmacol 69:86–94
Naz S, Imran M, Rauf A et al (2019) Chrysin (2019): Pharmacological and therapeutic properties. Life Sci 235:116797
Noor KK, Ijaz MU, Ehsan N, Tahir A, Yeni DK, Zihad SNK, Uddin SJ, Ashraf A, Simal-Gandara J (2022) Hepatoprotective role of vitexin against cadmium-induced liver damage in male rats: A biochemical, inflammatory, apoptotic and histopathological investigation. Biomed Pharmacother 150:112934
Oh C-M, Oh I-H, Lee J-K, Park YH, Choe B-K, Yoon T-Y, Choi J-M (2014) Blood cadmium levels are associated with a decline in lung function in males. Environ Res 132:119–125
Oh S, Yang J, Park C, Son K, Byun K (2021) Dieckol attenuated glucocorticoid-induced muscle atrophy by decreasing NLRP3 inflammasome and pyroptosis. Int J Mol Sci 22:8057
Paithankar JG, Saini S, Dwivedi S, Sharma A, Chowdhuri DK (2021) Heavy metal associated health hazards: An interplay of oxidative stress and signal transduction. Chemosphere 262:128350
Pan S, Wang Q, Zhang Q, Zhou M, Li L, Zhou X (2021) A novel circular RNA, circPUS7 promotes cadmium-induced transformation of human bronchial epithelial cells by regulating Kirsten rat sarcoma viral oncogene homolog expression via sponging miR-770. Metallomics 13:mfab043
Placer ZA, Cushman LL, Johnson BC (1966) Estimation of product of lipid peroxidation (malonyl dialdehyde) in biochemical systems. Anal Biochem 16:359–364
Poli V, Madduru R, Aparna Y, Kandukuri V, Motireddy SR (2022) Amelioration of cadmium-induced oxidative damage in wistar rats by Vitamin C, zinc and N-acetylcysteine. Medical Sciences 10:7
Rafiei-Asl S, Gh K, Jamshidian J, Rezaie A (2021) Protective effects of bromelain against cadmium-induced pulmonary intoxication in rats: a histopathologic and cytologic study. Arch Razi Inst 76:1427
Sedlak J, Lindsay RH (1968) Estimation of total, protein-bound, and nonprotein sulfhydryl groups in tissue with Ellman's reagent. Anal Biochem 25:192–205
Seydi E, Rahimpour Z, Salimi A, Pourahmad J (2019) Selective toxicity of chrysin on mitochondria isolated from liver of a HCC rat model. Bioorg Med Chem 27:115163
Sharaf El-Din AA, Abd Allah OM (2016) Impact of olmesartan medoxomil on amiodarone-induced pulmonary toxicity in rats: focus on transforming growth factor-ß1. Basic Clin Pharmacol Toxicol 119:58–67
Soliman MM, Aldhahrani A, Ghamry HI, Albogami S, Youssef GB, Kesba H, Shukry M (2022) Chrysin abrogates gibberellic acid-induced testicular oxidative stress and dysfunction via the regulation of antioxidants and steroidogenesis-and apoptosis-associated genes. J Food Biochem 46:e14165
Sun Y, Oberley LW, Li Y (1988) A simple method for clinical assay of superoxide dismutase. Clin Chem 34:497–500
Sun H, Hu H, Xu X, Fang M, Tao T, Liang Z (2021) Protective effect of dexmedetomidine in cecal ligation perforation-induced acute lung injury through HMGB1/RAGE pathway regulation and pyroptosis activation. Bioengineered 12:10608–10623
Talebi M, Talebi M, Farkhondeh T et al (2021) An updated review on the versatile role of chrysin in neurological diseases: Chemistry, pharmacology, and drug delivery approaches. Biomed Pharmacother 141:111906
Temel Y, Çağlayan C, Ahmed BM, Kandemir FM, Çiftci M (2021) The effects of chrysin and naringin on cyclophosphamide-induced erythrocyte damage in rats: biochemical evaluation of some enzyme activities in vivo and in vitro. Naunyn Schmiedebergs Arch Pharmacol 394:645–654
Turk E, Kandemir FM, Yildirim S, Caglayan C, Kucukler S, Kuzu M (2019) Protective effect of hesperidin on sodium arsenite-induced nephrotoxicity and hepatotoxicity in rats. Biol Trace Elem Res 189:95–108
Varışlı B, Darendelioğlu E, Caglayan C, Kandemir FM, Ayna A, Genç A, Kandemir Ö (2022) Hesperidin attenuates oxidative stress, inflammation, apoptosis, and cardiac dysfunction in sodium fluoride-Induced cardiotoxicity in rats. Cardiovasc Toxicol 22:727–735
Varışlı B, Caglayan C, Kandemir FM, Gür C, Ayna A, Genç A, Taysı S (2023) Chrysin mitigates diclofenac-induced hepatotoxicity by modulating oxidative stress, apoptosis, autophagy and endoplasmic reticulum stress in rats. Mol Biol Rep 50:433–442
Wang J, Zhang Y, Fang Z, Sun L, Wang Y, Liu Y, Xu D, Nie F, Gooneratne R (2019) Oleic acid alleviates cadmium-induced oxidative damage in rat by its radicals scavenging activity. Biol Trace Elem Res 190:95–100
Wang J, Ding L, Wang K, Huang R, Yu W, Yan B, Wang H, Zhang C, Yang Z, Liu Z (2022) Role of endoplasmic reticulum stress in cadmium-induced hepatocyte apoptosis and the protective effect of quercetin. Ecotoxicol Environ Saf 241:113772
Wang W-J, Lu X, Li Z, Peng K, Zhan P, Fu L, Wang Y, Zhao H, Wang H, Xu D-X (2023a) Early-life cadmium exposure elevates susceptibility to allergic asthma in ovalbumin-sensitized and challenged mice. Ecotoxicol Environ Saf 255:114799
Wang X, Xing C, Li G, Dai X, Gao X, Zhuang Y, Cao H, Hu G, Guo X, Yang F (2023b) The key role of proteostasis at mitochondria-associated endoplasmic reticulum membrane in vanadium-induced nephrotoxicity using a proteomic strategy. The Science of the Total Environment 869:161741
Wen S, Wang L, Zhang C, Song R, Zou H, Gu J, Liu X, Bian J, Liu Z, Yuan Y (2022) PINK1/Parkin-mediated mitophagy modulates cadmium-induced apoptosis in rat cerebral cortical neurons. Ecotoxicol Environ Saf 244:114052
Yardım A, Kandemir FM, Çomaklı S, Özdemir S, Caglayan C, Kucukler S, Çelik H (2021) Protective effects of curcumin against paclitaxel-induced spinal cord and sciatic nerve injuries in rats. Neurochem Res 46:379–395
Yesildag K, Gur C, Ileriturk M, Kandemir FM (2022): Evaluation of oxidative stress, inflammation, apoptosis, oxidative DNA damage and metalloproteinases in the lungs of rats treated with cadmium and carvacrol. Molecular Biology Reports, 1–11
Yu W, Tao M, Zhao Y, Hu X, Wang M (2018) 4′-Methoxyresveratrol alleviated AGE-induced inflammation via RAGE-mediated NF-κB and NLRP3 inflammasome pathway. Molecules 23:1447
Zhang C, Lin T, Nie G, Hu R, Pi S, Wei Z, Wang C, Li G, Hu G (2021) In vivo assessment of molybdenum and cadmium coinduce nephrotoxicity via causing calcium homeostasis disorder and autophagy in ducks (Anas platyrhyncha). Ecotoxicol Environ Saf 230:113099
Zhang W, Sun X, Qi X, Liu X, Zhang Y, Qiao S, Lin H (2022a) Di-(2-Ethylhexyl) Phthalate and Microplastics Induced Neuronal Apoptosis through the PI3K/AKT Pathway and Mitochondrial Dysfunction. J Agric Food Chem 70(35):10771–10781
Zhang W, Xu M, Wen S, Wang L, Zhang K, Zhang C, Zou H, Gu J, Liu X, Bian J (2022b) Puerarin alleviates cadmium-induced rat neurocyte injury by alleviating Nrf2-mediated oxidative stress and inhibiting mitochondrial unfolded protein response. Ecotoxicol Environ Saf 247:114239
Zhang W, Yin K, Shi J, Shi X, Qi X, Lin H (2022c) The decrease of selenoprotein K induced by selenium deficiency in diet improves apoptosis and cell progression block in chicken liver via the PTEN/PI3K/AKT pathway. Free Radical Biol Med 189:20–31
Zhang W, Sun X, Shi X, Qi X, Shang S, Lin H (2023) Subacute Cadmium Exposure Induces Necroptosis in Swine Lung via Influencing Th1/Th2 Balance. Biol Trace Elem Res 201(1):220–228

Zhou Z, Lu Q, Huang Q, Zheng C, Chen B, Lei Y (2016) eIF3 regulates migration, invasion and apoptosis in cadmium transformed 16HBE cells and is a novel biomarker of cadmium exposure in a rat model and in workers. Toxicology Research 5:761–772

Zhu L, Duan P, Hu X, Wang Y, Chen C, Wan J, Dai M, Liang X, Li J, Tan Y (2019) Exposure to cadmium and mono-(2-ethylhexyl) phthalate induce biochemical changes in rat liver, spleen, lung and kidney as determined by attenuated total reflection-Fourier transform infrared spectroscopy. J Appl Toxicol 39:783–797